ELSEVIER

Materials Science and Engineering B80 (2001) 125–129

MATERIALS SCIENCE & ENGINEERING B

www.elsevier.com/locate/mseb

Study of Zn diffusion in n-type GaSb by cathodoluminescence and scanning tunneling spectroscopy

P. Hidalgo [a], B. Méndez [a], J. Piqueras [a,*], P.S. Dutta [b]

[a] *Departamento de Física de Materiales, Facultad de Físicas, Universidad Complutense, 28040 Madrid, Spain*
[b] *Department of Electrical, Computer and Systems Engineering, Rensselaer Polytechnic Institute, Troy, NY 12180-3590, USA*

Abstract

We report here the studies carried out in zinc diffused n-type GaSb by cathodoluminescence (CL) microscopy and by scanning tunneling spectroscopy. Samples with different diffusion profiles measured by secondary ion mass spectrometry (SIMS) were obtained. CL plan-view observations show high homogeneity in the diffused layers. Cross-sectional measurements of the Zn diffused layers were performed by current imaging tunneling spectroscopy (CITS). The junction border was revealed clearly in the CITS images and conductance spectra recorded at differents points of the layers provided information on the local surface band gaps and the conductive behaviour. The results were related to the diffusion profiles and were found to agree with diffusion models suggested previously.

Keywords: Scanning tunneling spectroscopy; Diffusion; Gallium antimonide; Junctions

1. Introduction

GaSb and related compounds are of large interest for many optoelectronic devices operating in the infrared range. LEDs and photodiodes based on other III–V compounds, as the GaAsP system, are routinely fabricated by the formation of diffused p–n junctions [1]. In particular, Zn diffusion in n-type material has been employed to form p–n junctions to be used in optoelectronic devices like solar cells or laser diodes. The dopant concentration profile in the near surface region of the diffused junctions plays a significant role in the optical and electrical performance of the devices [2,3]. However, there is limited work in the literature on GaSb homojunctions. Consequently, investigation on the recombination properties in the diffused layer and the depth resolved conductance behaviour is essential to predict accurately the resulting Zn diffusion profiles.

In this work, we have used a pseudo-closed box diffusion system to diffuse Zn into Te-doped GaSb substrates to form p–n junctions. This diffusion technique yields good control over Zn surface concentration and junction depth [4]. The recombination properties of the diffused layers were investigated by cathodoluminescence (CL) in the scanning electron microscope (SEM) and the depth resolved conduction type was studied by current imaging tunneling spectroscopy (CITS). The results were correlated with diffusion profiles measured by Secondary Ion mass spectrometry (SIMS).

2. Experimental method

Te-doped n-type GaSb single crystalline wafers with electron concentrations of about 2×10^{17} cm^{-3} were diffused with Zn in two different ways to form p–n junctions. Samples labelled as p–n-1 were diffused by the spin on glass technique for 2 h at 650°C. Samples labelled as p–n-2 were diffused from a vapour phase in a pseudo-closed box system. The diffusion time was also 2 h and the temperature 500°C. The diffusion profiles were measured by using SIMS technique. We have also investigated an undiffused wafer as a reference sample.

CL measurements were carried out using a Hitachi S-2500 SEM at 77 K at beam energies of 10–25 keV, with a cooled ADC germanium detector. The details of

* Corresponding author. Tel.: +34-91-3944561, fax: +34-91-3944547.
E-mail address: piqueras@eucmax.sim.ucm.es (J. Piqueras).

0921-5107/01/$ - see front matter
PII: S0921-5107(00)00635-8

the experimental set up for recording images and spectra are described elsewhere [5]. For the scanning tunneling microscopy (STM) measurements a combined SEM/STM based on a Leica S440 SEM operating under vacuum of 10^{-6} Torr was used. The small size of the STM enabled it to be mounted on the SEM specimen holder. The main features of this system are similar to those described in [6]. Electrochemically etched or mechanically sharpened Pt–Ir and Au wires were used as probe tips. For CITS measurements the constant current image was obtained in a 128×128 pixel grid, the feedback loop interrupted for 2 ms, and the voltage digitally ramped from the tunnel voltage to a set of 44 predetermined values while the current was sampled. This provides 44 tunneling current files at different voltages. To analyze the data, the normalized differential conductance, (dI/dV)/(I/V), spectra were recorded. These curves give information directly related to the superficial density of states and also give the value of the energy gap at the surface [7]. The samples for STM were cleaned in hydrochloric acid and acetone, dried in a flow of dry nitrogen, and inmediately mounted in the microscope chamber. The combined setup SEM/STM enables us to position the tip of the STM in the neighbourhood of the junction border. First, we have studied the characteristics of the reference sample. Secondly, we have examined the surface of the p regions in both diffused samples. Finally, a cross-section of the sample p–n-2 was prepared and local information at differents points near the junction limit was achieved.

3. Results and discussion

The SIMS profiles are shown in Fig. 1. In sample p–n-1 a surface layer of 250 nm thickness is formed with a relatively slow decrease of Zn concentration from 2 to 1×10^{19} cm^{-3} followed by a sharp diffusion front. In sample p–n-2, the diffused region shows a first plateau with a Zn concentration of 10^{20} cm^{-3} followed by a kink at 550 nm and a second plateau with a Zn concentration of 10^{19} cm^{-3} that reaches to 1000 nm below the surface. Although no models of Zn diffusion have been to our knowledge suggested for GaSb, it is reasonable to assume that the diffusion mechanisms of Zn in GaAs and GaSb are similar. The profile obtained in sample p–n-1 can be explained by the standard interstitial-substitutional diffusion mechanism, which is usually used to model Zn diffusion in III–V materials [8] where interstitial zinc reacts with a gallium vacancy to form a substitutional zinc acceptor. The anomalous shape of the zinc diffusion profile of sample p–n-2 has also been reported in diffused junction GaSb solar cells [9]. To explain the appearance of kinks in the Zn diffusion profile in GaAs, Reynolds et al. [10] suggested that the kink may be caused by the existence of two mobile Zn species, which dominate in different regions according to the position of the Fermi level. Alternatively, a model involving multiple ionization states for gallium vacancies has also been proposed [11].

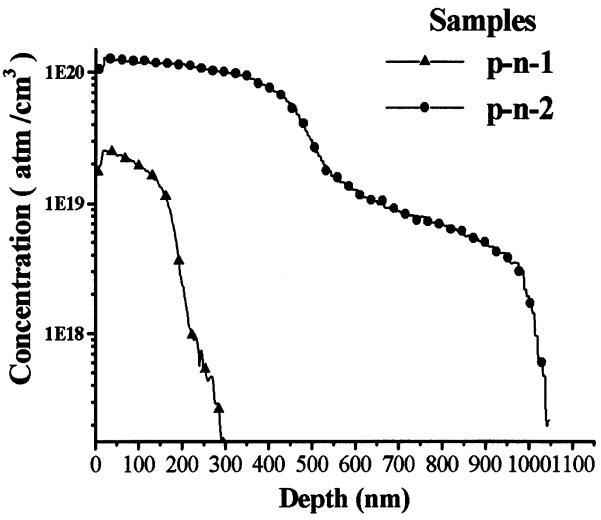

Fig. 1. SIMS profiles of Zn concentration after Zn diffusion in Te-doped GaSb.

CL images from the undiffused GaSb–Te substrate reveal inhomogeneities in the distribution of radiative recombination centres. The main observed features are striations due to dopant fluctuations and dark spots related to isolated defects (Fig. 2). These images are similar to that obtained in other III–V semiconductors like GaAs–Te [12]. In Te-doped GaSb, it has also been found that periodic variations in CL intensity, spatially correlated with growth striations, corresponds to changes in carrier concentration [13]. CL spectra recorded from the reference sample (Fig. 3) show three main emission bands corresponding to the near band edge emission at 795 meV, the native defects related band at 777 meV and the Te related band at 746 meV. The 777 meV peak is usually present in GaSb and has been attributed to a transition from conduction band to the native acceptor level $V_{Ga}Ga_{Sb}$ [14]. The centre responsible for the 746 meV emission could be the complex defect $V_{Ga}Ga_{Sb}Te_{Sb}$ as it has been suggested previously in this range of Te doping [15,16]. The monochromatic images from this emission show a contrast of parallel lines corresponding to the above mentioned striations. On the other hand, the monochromatic images from the 777 meV band are featureless indicating a homogeneous distribution of native defects in the sample.

After Zn diffusion, plan view CL images do not reveal inhomogeneities in the diffused region in both samples. These results indicate that the defects in the layers are either present with low concentration or are not electrically active, which implies a high quality of the layers for device applications. CL spectra from the

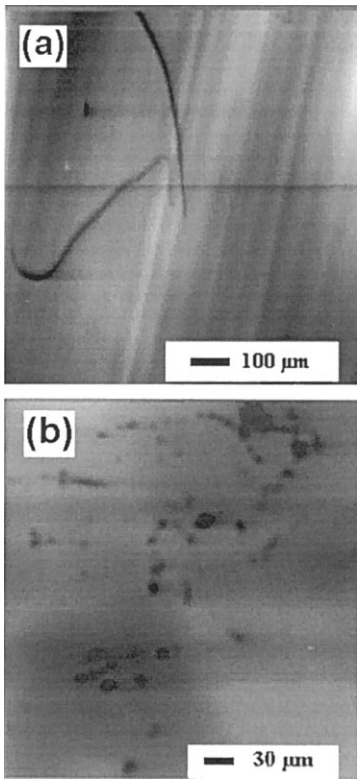

Fig. 2. CL images obtained from the reference Te-doped GaSb sample in which (a) striations are observed and (b) dark spots related to isolated defects.

p-region in the two samples show a slight quenching of the native defect related band, while the main emission corresponds to the center involving Te. The presence of Zn in the layers is not revealed readily through the CL spectra due to the fact that the Zn related emission peak at 770 meV [17] is very close to the intense 777 meV defect band.

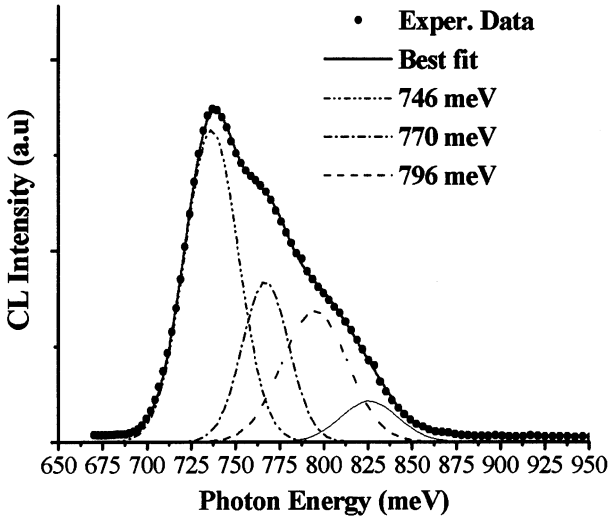

Fig. 3. CL spectrum of the reference Te-doped GaSb sample. Broken lines show Gaussian bands that best fit the experimental data.

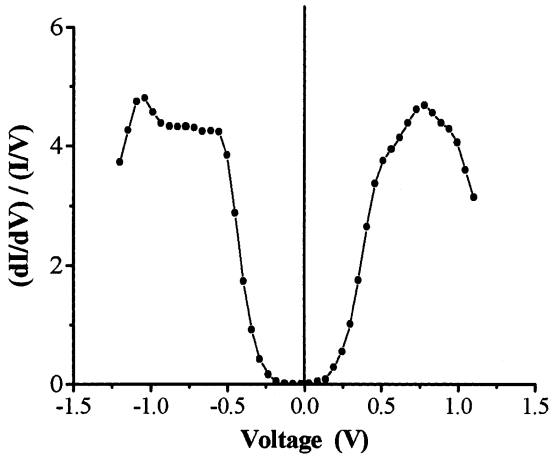

Fig. 4. Typical normalized differential conductance spectrum recorded in the control sample.

In order to study the local electronic properties in the layers CITS measurements have been performed and curves of normalized differential conductance were obtained. The curves were plotted from the data of the CITS images corresponding to the 44 selected voltage values by averaging the data on regions of about 10×10 nm. Fig. 4 shows a typical normalized conductance differential spectrum obtained in the reference sample. The band gap value measured from the spectrum is about 0.5 eV, which is lower than the bulk band gap (0.8 eV). Previous works on CITS measurements of doped GaSb [18,19] revealed surface band gap values similar to that observed here for Te-doped material. The position of the zero bias voltage, which corresponds to the Fermi level, indicates the n-type conduction of the sample. CITS images of all examined areas show slight contrast due to local conductance variations with a spatial resolution in the range 1–10 nm.

Also the CITS images from diffused samples do not show significantly contrast due to inhomogenities in local conductivity. The sample surface after Zn diffusion remains smooth. The conductance spectrum obtained from the diffused layer in sample p–n-1 is shown in Fig. 5. In this case, the surface band gap value is about 0.2–0.3 eV, which is lower than in the reference sample, and the position of the Fermi level is near the middle of the gap. A decrease in the band gap value is expected due to the rather high Zn concentration (10^{19} cm^{-3}) at the surface shown by SIMS data. Fig. 6 shows the differential conductance spectrum from the diffused layer in sample p–n-2. The high Zn concentration (10^{20} cm^{-3}) at the surface leads to a narrow band gap and the position of the zero-bias voltage shows clearly the p-type behaviour of this surface.

In order to study the depth resolved conductance behaviour in the diffused layer a cross-section of the p–n-2 sample was investigated. The junction border was clearly imaged by STM at a depth of 1 μm, in

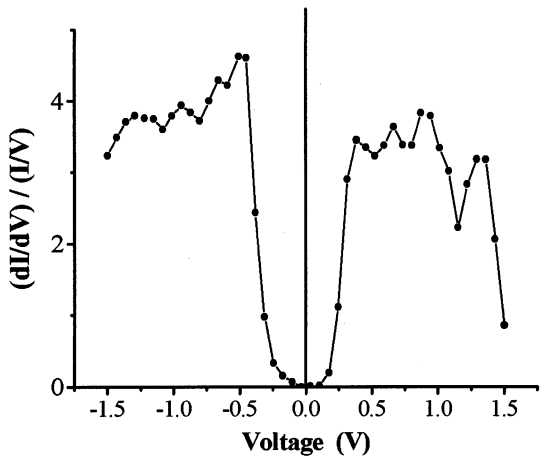

Fig. 5. Normalized differential conductance spectrum recorded at the Zn diffused surface in sample p–n-1.

agreement with the SIMS measurements. Fig. 7 shows a constant current image and corresponding CITS images of the junction obtained at $+0.5$ and -0.5 V, respectively. In these images, a rather curved limit is shown while a sharper boundary is observed at higher magnification. With the aid of the SEM, the tip of the STM was situated at different points near the junction border and conductance spectra from the region corresponding to the second plateau in the SIMS profile were obtained. The measurements performed at these positions revealed a band gap value of about 0.2–0.3 V and a shift of the Fermi level towards the middle of the gap. These results agree with the models proposed to explain the anomalous Zn diffusion profile in GaAs [10] in which the existence of two different diffusion species (Zn^{+} and Zn^{++} insterstitials) depending on the Fermi level, are the responsible for the appearance of two plateaux in the SIMS profile. In GaSb, the Zn diffusion

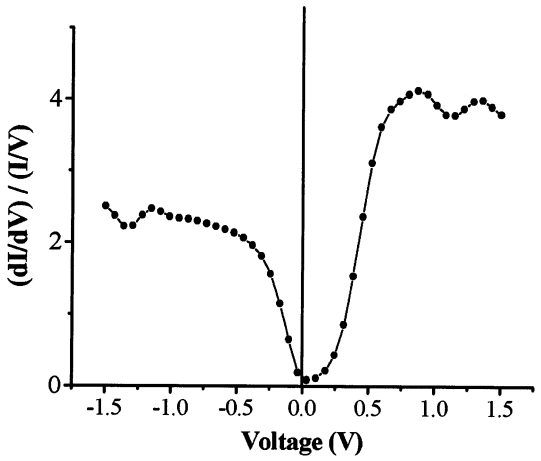

Fig. 6. Normalized differential conductance spectrum recorded at the Zn diffused surface in sample p–n-2.

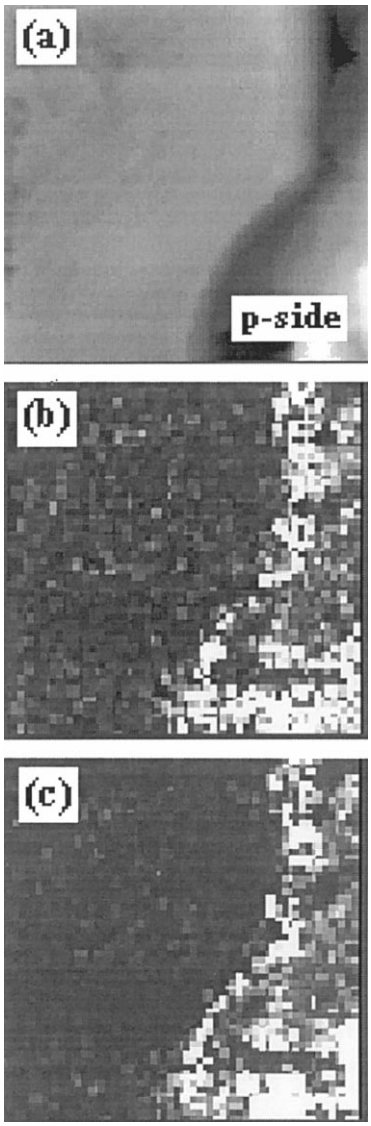

Fig. 7. 1.5×1.5 μm^2 STM image of zinc diffused cross-section in Te-doped GaSb p–n-2 sample. (a) Topography image acquired with a sample voltage of $+0.75$ V and 0.5 nA tunneling current. (b) Corresponding CITS image obtained at $+0.5$ V. (c) CITS image obtained at -0.5 V.

mechanisms should be similar. According to this model, Zn^{++} would be formed at the surface and dominate the diffusion process in the heavily doped surface region, while the more mobile Zn^{+} is dominant in the less heavily doped region near the diffusion front. The corresponding conductance spectra we have obtained from the cross-section in sample p–n-2 show a displacement in the position of the Fermi level as is suggested in [10]. The shape of the conductance spectra was moreover influenced by the Zn concentration. The possibility to form complexes involving Zn interstitials with point defects seems to be ruled out at the sight of the homogeneity in CL images.

4. Conclusions

p–n Junctions formed by zinc diffusion in Te-doped GaSb were studied by CL and scanning tunneling spectroscopy. The diffused layers were found to be very homogeneous in plane-view CL images which is important for device applications. In one of the junctions, a double profile was obtained as shown by SIMS measurements. A tunneling current image of a cross-section reveals the junction border at a depth in agreement with SIMS results. Study of local conductance spectra in the cross-section enabled us to detect the two plateaux obtained through the SIMS data and to confirm experimentally the modified interstitial-substitutional standard model for Zn diffusion in GaSb.

Acknowledgements

This work was supported by DGES (Project PB96-0639).

References

[1] A. Usami, Y. Tokuda, H. Shiraki, H. Ueda, T. Wada, H. Kan, T. Murakami, J. Appl. Phys. 66 (1989) 3590.
[2] P.E. Gruenbaum, V.T. Dinh, V.S. Sundaram, Solar Energy Mater. Solar Cells 32 (1994) 61.
[3] O. Shulima, A. Bett, 11th International Photovoltaic Science and Engineering Conference, Sapporo, Japan, 1999.
[4] A.W. Bett, S. Keser, O.V. Sulima, J. Crystal. Growth 181 (1997) 9.
[5] B. Méndez, J. Piqueras, J. Appl. Phys. 69 (1991) 2776.
[6] A. Asenjo, A. Buendía, J.M. Gómez-Rodríguez, A. Baró, J. Vac. Sci. Technol. B12 (1994) 1658.
[7] R.M. Feenstra, J.A. Stroscio, A.P. Fein, Surf. Sci. 181 (1987) 295.
[8] L. Weisberg, J. Blanch, Phys. Rev. 131 (1963) 1548.
[9] V.S. Sundaram, P.E. Gruenbaum, J. Appl. Phys. 73 (1993) 3787.
[10] S. Reynolds, D.W. Vook, J.F. Gibbons, J. Appl. Phys. 63 (1988) 1052.
[11] K.B. Kahen, Appl. Phys. Lett. 55 (1989) 2117.
[12] B. Méndez, J. Piqueras, F. Domínguez-Adame, N. De Diego, J. Appl. Phys. 64 (1988) 4466.
[13] A.K. Chin, W.A. Bonner, Appl. Phys. Lett. 40 (1982) 248.
[14] M.C. Wu, C.C. Chen, J. Appl. Phys. 72 (1992) 4275.
[15] A.I. Lebedev, I.A. Strel'nikova, Sov. Phys. Semicond. 13 (1979) 229.
[16] P.S. Dutta, B. Méndez, J. Piqueras, E. Dieguez, H.L. Bhat, J. Appl. Phys. 80 (1996) 1112.
[17] P.S. Dutta, K.S.R. Koteswara Rao, H.L. Bhat, V. Kumar, Appl. Phys. A 61 (1995) 149.
[18] P. Hidalgo, B. Méndez, J. Piqueras, P.S. Dutta, E. Dieguez, Phys. Rev. B 60 (1999) 10613.
[19] P. Hidalgo, B. Méndez, J. Piqueras, J. Plaza, E. Dieguez, J. Appl. Phys. 86 (1999) 1449.